The A. B. Wood Medal paper

High frequency seabed scattering and sediment discrimination

G. J. Heald

Defence Evaluation and Research Agency, Newton Road, Weymouth, Dorset, DT3 5BQ, UK.
gjheald@dera.gov.uk

Abstract

The use of first and second normal incidence backscatter from the seabed for sediment discrimination is discussed and it is shown that the second echo must be treated in terms of an on-axis bistatic geometry. It is also shown that the bistatic geometry is the reason why the second echo contains additional information. The importance of the water surface roughness is also discussed. A tank experiment using a 215 kHz transducer, three sediment types and various level of water surface roughness is used to show the level of sediment discrimination and comparison with the theoretical predictions.

1. Introduction

The use of high frequency acoustic scattering has been of interest over many years and for many applications the backscatter of sound from the ocean boundaries has been the dominant background signal which hampers the detection of objects that lie within the reverberant field. Other areas of the sonar community have exploited the scattering of sound from the sediment to provide a measure of the depth below the keel of a vessel to ensure safe passage in coastal waters. This has been achieved using echo-sounders which are designed for use at normal incidence to the sea-floor and are generally mounted in the hull of the host vessel. Examples of such systems can be found on vessels ranging from small pleasure craft up to the largest commercial liners and tankers. In recent years researchers have studied the characteristics of the received signal to exploit them for sediment classification.

In the late 1980's a system was developed known as RoxAnn [1-3] which used the first and second echo from the seabed to provide a "sediment classification". The second echo is the signal which has been scattered from the sediment up to the echosounder where it is then scattered from the sea surface back towards the seabed, and finally scattered for a second time and received at the echo sounder. The development of RoxAnn was based on a previous report of normal incidence multiple echoes, resulting from a number of ocean experiments that had been conducted by Orlowski [4]. The path for the second echo is illustrated in Figure 1 and will be discussed in detail during the following sections. The insonification radius for the second backscatter is three time the radius of the first backscatter.

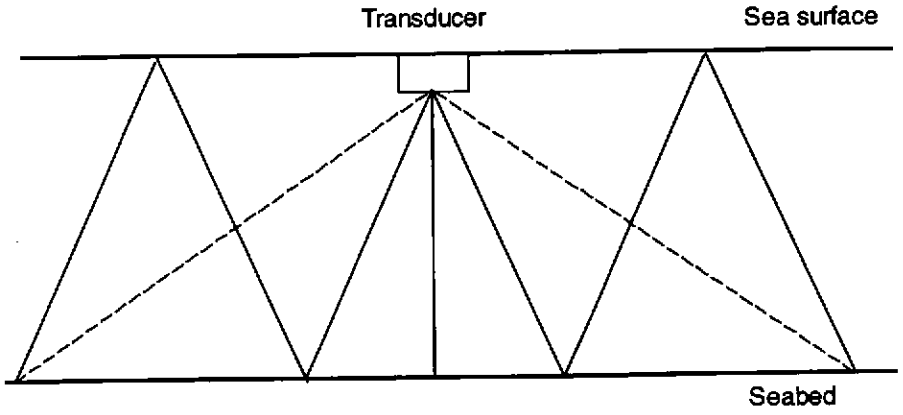

Figure 1. The signal path for the second insonification of the seabed (solid line) and the return path to the receiver (dashed line).

The authors of [1-3] claimed that if the first echo were integrated over its tail (denoted E_1) and the whole of the second echo was integrated (denoted E_2) the resulting plot of E_2 against E_1 meant that different sediment type fell into different regions of the graph. Hard rough seabed types had high E_1 and E_2 whereas smooth soft sediments resulted in low values of E_1 and E_2. This had been observed empirically but there was no theoretical

derivation provided to show why the second echo should contain new information. The designers of RoxAnn had also denoted the E_1 axis as the a measure of roughness and the E_2 axis as hardness. Understanding the physical mechanisms involved in this process provided the motivation for the research that is presented here.

Section 2 of this paper presents the theoretical equations for the first and second backscatter intensity using the high frequency limit of the Helmholtz-Kirchhoff integral. As will be shown, the second backscatter must be treated as a bistatic, on-axis geometry with the source at an effective range of three times the water depth, whereas the receiver is still only at one water depth from the sediment. Treating the second echo in this way also provides insight into the mechanisms giving additional information that is not available in the first backscatter. Pace *et al.* [5] have shown that if a receiver is moved closer to a rough scattering surface, with the source fixed at a given range, the receiver will move from the farfield scattering zone and into the near-field zone. As the range ratio of source and receiver was increased, it was also shown that the backscattered strength becomes proportional to the image solution and less dependant on the surface roughness. A simple extension to the theory is included, at the end of Section 2, to take account of the spreading due to the water surface roughness. This may also increase the effective separation ratio of the source and receiver thus enhancing the techniques.

Sections 3 and 4 present a tank experiment that was conducted to investigate the first and second backscatter. A 215 kHz transducer was used as the source and receiver with its axis at normal incidence to the floor of the tank. The experiments included 3 sediments, a water surface wave generator and a two probe wave measuring system for measuring the wave roughness. The transducer was mounted on a computer controlled gantry to allow accurate positioning over each of the sediment trays. The results obtained from the range of sediments, with different water surface roughness conditions, are plotted as E_2 against E_1. Example of the time series intensities, with the theoretical prediction overlaid, are given in Section 3.

2. Theory

The theory for the first echo is developed to provide the ensemble average time-series backscattered intensity for the region where the insonified area has become an annulus (i.e. the tail) and the second echo is developed with limits applied to provide the time-series for the rising edge and the tail as these are required for derivation of E_2. In each case the surface roughness and beam function is assumed to be Gaussian. The rms height and correlation length, at the e^{-1} contour, are then used to determined the rms slope of the surface. At high frequencies the penetration into the sediment can safely be ignored. A companion paper [6] in these proceedings extends the theory to lower frequencies (1–10 kHz) and includes the effect of the sediment volume scatter and a sub-bottom layer.

2.1 The First Backscatter

The intensity for the first backscatter must include the effect of scattering and reflection of the incident signal on the rough interface, the beam response of the source and receiver and the range of the transducer from the sediment interface. Throughout the development of the theory it has been assumed that the transducer is at the water surface, although the theory is still applicable if the transducer is below the surface. The geometry is shown in Figure 2.

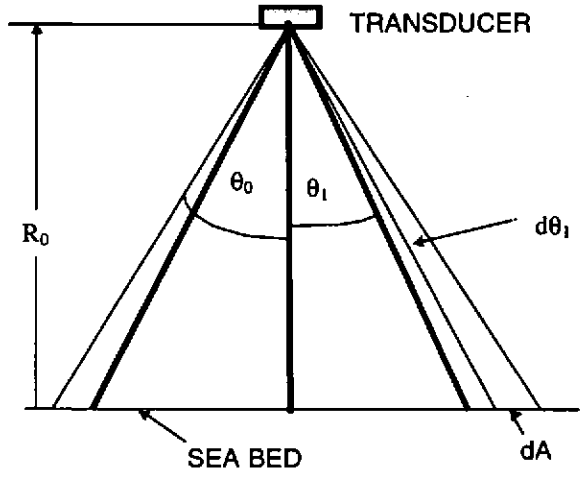

Figure 2. Geometry for the first backscatter

The resulting integral for the first backscatter intensity can be written as:

$$I_{bs1} = I_0 \int_{\theta_a}^{\theta_b} \frac{S_1(\theta_1) G^2(\theta_1)}{(R'_0)^4} dA \tag{1}$$

where

$$dA = 2\pi R'^2_0 \tan\theta_1 \, d\theta_1 \tag{2}$$

$$R'_0 = R_0 \sqrt{(1 + \tan^2\theta_1)} \tag{3}$$

I_0 is the source intensity at a distance of 1m from the source and the limits are time functions discussed below.

The backscattering coefficient $S_1(\theta_1)$ resulting from the high frequency limit solution to the Helmholtz-Kirchhoff integral (assuming a Gaussian surface) is given by Brekovskikh and Lysanov [7] and repeated by Pace [8] and may be written as:

$$S_1(\theta_1) = \frac{\Re^2 T^2}{32\pi h^2} \left(\frac{\exp\left(-\left(\frac{T \tan\theta_1}{2h} \right)^2 \right)}{\cos^4\theta_1} \right) \tag{4}$$

h is the rms height of the surface roughness, T is the rms correlation length of the surface roughness and $\Re$ is the plane wave reflection coefficient. The scattering function is thus dependant on the rms slope of the sediment, as it contains both the rms height (h) and the rms correlation length (T).

The source and the receiver both have the same Gaussian beam pattern function $G(\theta_1)$ and:

$$G^2(\theta_1) = G_t G_r = \exp\left(-2 \left(\frac{\tan^2\theta_1}{\tan^2\theta_0} \right) \right) \tag{5}$$

The region of interest for the first backscatter (t=0 corresponds to its arrival at the receiver) is the tail of the intensity envelope. This is the region where the insonified area on the seabed is an annulus, and occurs when

$$\frac{ct}{2} > \frac{c\tau}{2}$$

The limits of the integral θ_a and θ_b come from:

$$\sqrt{\frac{c(t-\tau)}{R_0}} \le \theta_1 \le \sqrt{\frac{ct}{R_0}}$$

and the solution to the integral for the intensity tail is:

$$I_{bs1} = \frac{M}{2\beta^2} exp\left(\frac{-\beta^2 ct}{R_0} \right) \left(\exp\left(\frac{\beta^2 c\tau}{R_0} \right) - 1 \right) \tag{6}$$

where

$$M = \frac{I_0 \Re^2 T^2}{16 h^2 R_0^2}, \quad \beta^2 = \frac{T^2}{4h^2} + \frac{2}{\tan^2\theta_0}$$

2.2 The second Backscatter

In order to understand the signal paths for the second backscatter it is necessary to treat the source as though it were at three times the water depth, as shown in Figure 3. This reveals that the geometry as no longer a simple monostatic case and the equation to represent this must be based on an "on-axis bistatic" geometry with the source at three times the water depth and the receiver at only one water depth. The ratio R_1/R_2 can be defined as α and as θ_1 and θ_2 are related this can be used reduce the integral. Over small angles it is valid to approximate tan θ with θ and this has been used in the development given here. The integral for I_{bs2} can be written as:

$$I_{bs2}=\frac{I_0\Re^4\beta_1^2}{4}\int_{\theta_1}^{\theta_2}\frac{\exp\left(-\beta_1^2\frac{\theta_1^2}{4}(1+\alpha)^2\right)\exp\left(-\beta_2^2\theta_1^2\right)}{R_2^2(1+\alpha^2\theta_1^2)}\theta_1 d\theta_1\left(1+\frac{\theta_1^2(1+\alpha)^2}{4}\right)^2 \quad (7)$$

where

$$\beta_1^2=\frac{T^2}{4h^2}$$

$$\beta_2^2=\frac{(1+\alpha^2)}{\tan^2\theta_0}$$

The reflection coefficient ($\Re$) term becomes $\Re^4$ as there have been two reflections from the sediment.

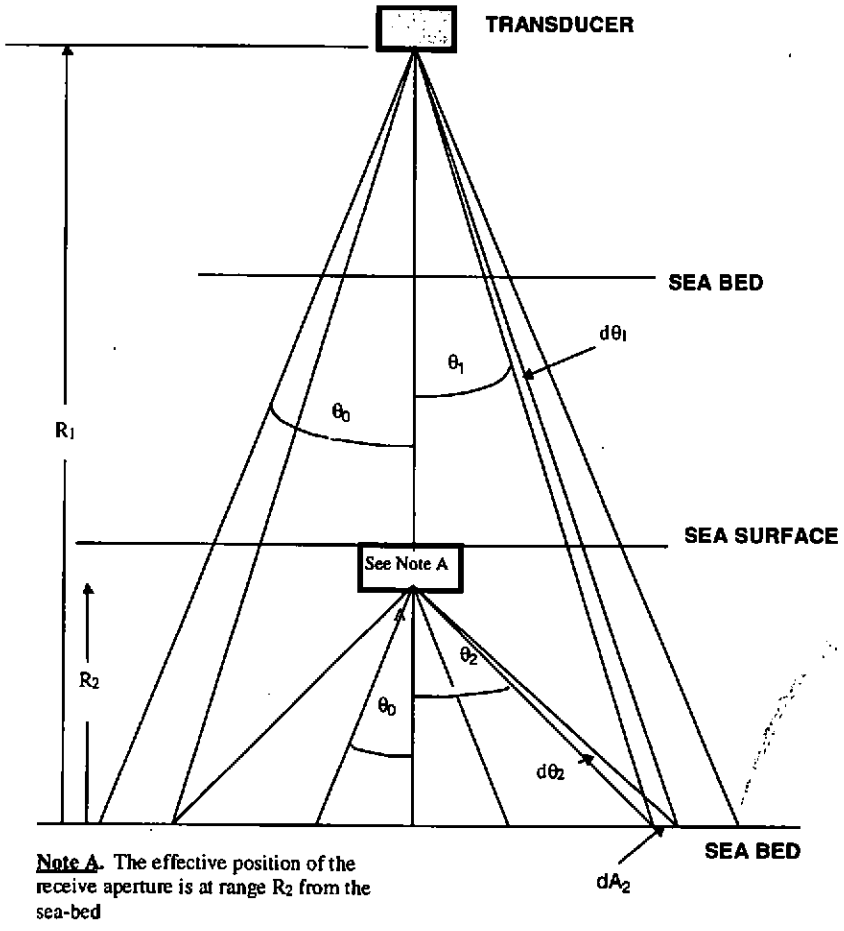

Figure 3. Expanded geometry for the second backscatter showing the effective range of the source as three times the water depth and receive range

The solution to the integral given in (7) is given below and involves retaining only the first two terms of the exponential integral function.

$$I_{bs2}=\frac{\pi\,\Re^4\beta_1^2}{4R_2^2\,\beta_4^2}\left[\exp(-x)\left(\left(\left[\frac{-1}{\left(x+\frac{1}{B_2}\right)}\right]+\left[\left[\frac{1}{\left(x+\frac{1}{B_2}\right)^2}\right]\right]\right)\left(1-\frac{2B_1}{B_2}+\frac{B_1^2}{B_2^2}\right)\exp\left(\frac{-1}{B_2}\right)+\left(\frac{-2B_1}{B_2}+\frac{B_1^2}{B_2^2}-\frac{xB_1^2}{B_2}-\frac{B_1^2}{B_2}\right)\right)\right]_{x_b}^{x_a} \quad (8)$$

where $$B_1 = \left(\frac{\beta_5}{\beta_4}\right)^2, \quad B_2 = \frac{\alpha^2}{\beta_4^2} \text{ and } \beta_5^2 = \frac{(1+\alpha)^2}{4}$$

The times series of the second backscatter must be treated in two separate parts in the following way:

Case 1. Full insonification. This is the region where $ct \le c\tau$ (τ = pulse length).

$$x_a = 0$$
$$x_b = \theta_a^2 \beta_4^2$$

Case 2. Annulus. This is the region where $ct > c\tau$.

$$x_a = \theta_a^2 \beta_4^2$$
$$x_b = (\theta_a + \delta\theta)\beta_4^2$$

2.3 Sea Surface Roughnness

The theory presented in the previous section assumes that there is no spreading due the roughness at the intermediate interfaces, which would not be the case if waves were present. This spreading also increases the insonified area for the second echo giving the apparent effect that the source receiver ratio has increased. The spreading at the interfaces can be represented by increasing the source beamwidth which means that a separate variable is required to represent source and receiver. This results in β_2^2 becoming:

$$\beta_2^2 = \frac{1}{\theta_0^2} + \frac{\alpha^2}{\phi_0^2} \tag{9}$$

where ϕ_0 is the half beamwidth of the source at the e^{-1} contour and θ_0 becomes the half beam width at the e^{-1} contour for the receiver only. The result of spreading on E_2 is shown in Figure 4 which shows an increased sensitivity to changes in reflection coefficient.

2.4 E1 and E2

The E_1 and E_2 values are obtained by integrating the tail of I_{bs1} and the whole of I_{bs2} respectively. This can be written as:

$$E_1 = \int_{t_1}^{t_2} I_{bs1}(t)\, dt \tag{10}$$

$$E_2 = \int_{0}^{t_3} I_{bs2}(t)\, dt + \int_{t_3}^{t_4} I_{bs2}(t)\, dt \tag{11}$$

Note that the two integrals are required for E_2 so that the integral includes the rising edge and the tail of the backscatter envelope. The lower limit starts at 0 which represents the time at the onset of the second echo. As both E_1 and E_2 are both integration of intensity over time they provide a measure of the energy in the respective regions of the backscatter envelopes.

Figure 4 shows a set of curves for a change in reflection coefficient of 0.1. The half beamwidth for the receiver was fixed as 10 degrees and the source half beamwidth was set at 10 , 15 and 30 degrees. The E_2 values were obtained using the equation presented in the previous sections. The receiver is simulated as moving from the monostatic position toward the sediment. It can be seen that, at the 20 m range, the difference between the E_2 value with the wider source beam-width (due to boundary spreading) is much greater than the case for the flat surface (i.e. source and receiver = 10°). The difference is also much larger than the change seen for the monostatic case in which the source and receiver are at an effective range of 60 metres.

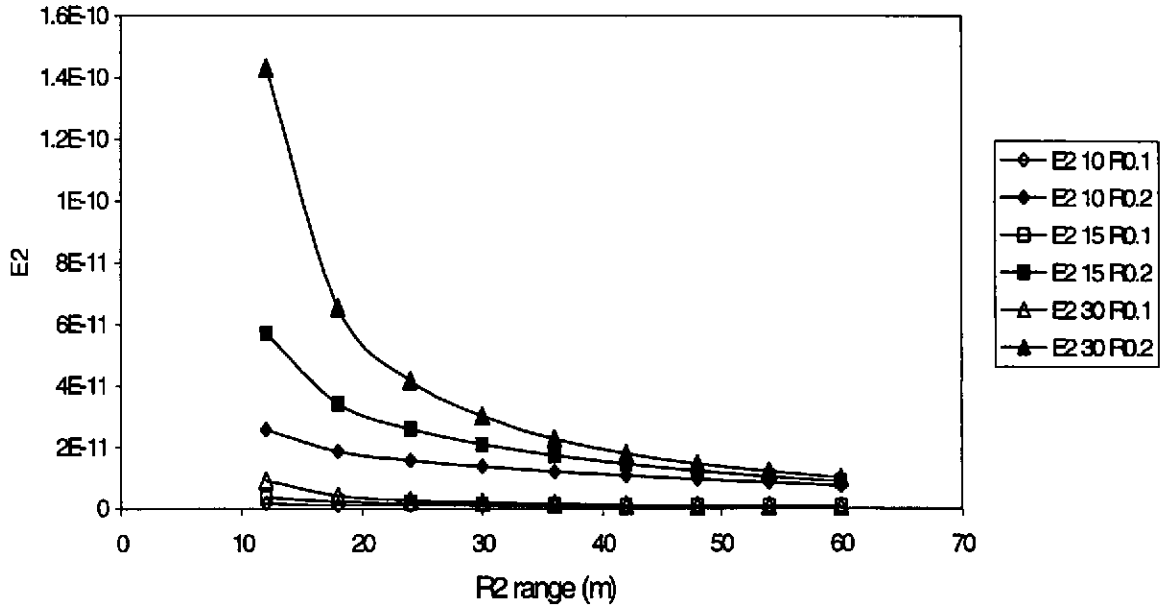

Figure 4. E_2 values computed at a range of source receiver separation with source half beam widths ϕ_0 of 10°, 15° and 30° and reflection coefficients of 0.1 and 0.2. The important receiver range in this study is 20m (i.e. 1/3 the source range).

3. Tank Experiment

In order to investigate the mechanisms that have been discussed in Section 2 a tank experiment was designed with three sediment types (Sand, Gravel and Pebbles) placed in metal trays on the tank floor. Each sediment tray was 1 m x 1.3 m x 0.3 m deep which was sufficient to gather data from 260 positions without any reflections from the tank walls. Data was gathered with three different water surface conditions: flat, small waves and large waves. The water depth was set to 1m and the 215 kHz transducer was fixed at a range of 0.95 m from the sediment. The pulse length used throughout the experiments was 100μs. Prior to starting the experiments the wave generator had been calibrated using a measuring probes fitted to a commercially available wave monitor. Details of the wave generation, measurement system and sediment roughness measurement are given in [9].

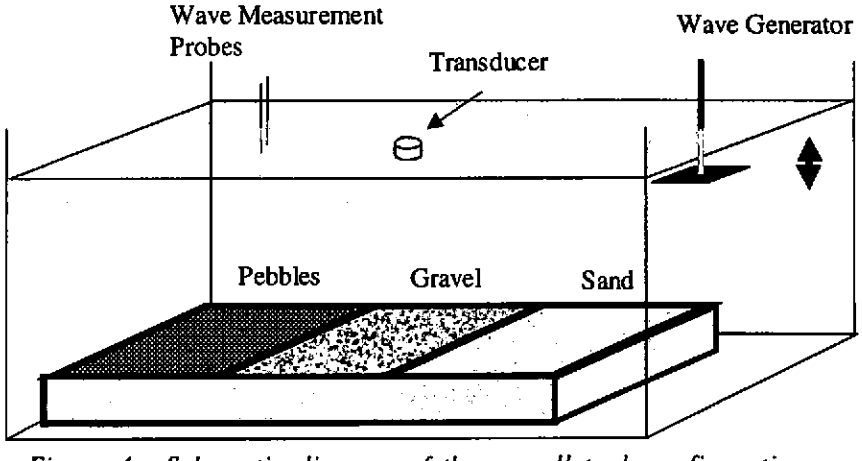

Figure 4. Schematic diagram of the overall tank configuration showing the end of the tank where the experiments were conducted

The backscatter at each position was used to form an ensemble average intensity envelope. Tests had shown that a stable average could be obtained using 5 adjacent positions to form the moving average. This resulted in 234 ensemble average envelopes of the first and second backscatter. In the cases where a moving water surface was present the second echo was recorded for 20 transmissions in each position so that the effect of the wave could be analysed.

The E_1 values were obtained by integrating over the tail of the first backscatter envelopes and the E_2 were obtained by integrating over the whole of the second backscatter. Care was taken during these experiments to ensure that the receive signal did not clip. This is not always the case in commercial echo-sounders as they have traditionally been designed for detection of the seabed rather than any concern for linearity. In such cases the integration for E_1 would need to be started some way down the envelope tail, as is the case in RoxAnn.

The values of the sediment roughness, transducer characteristics and surface wave were used to compare the predicted envelope with the measured envelope in each condition. An example of this comparison is given in Figure 5 which is for the gravel with small waves; a full analysis is available in [9].

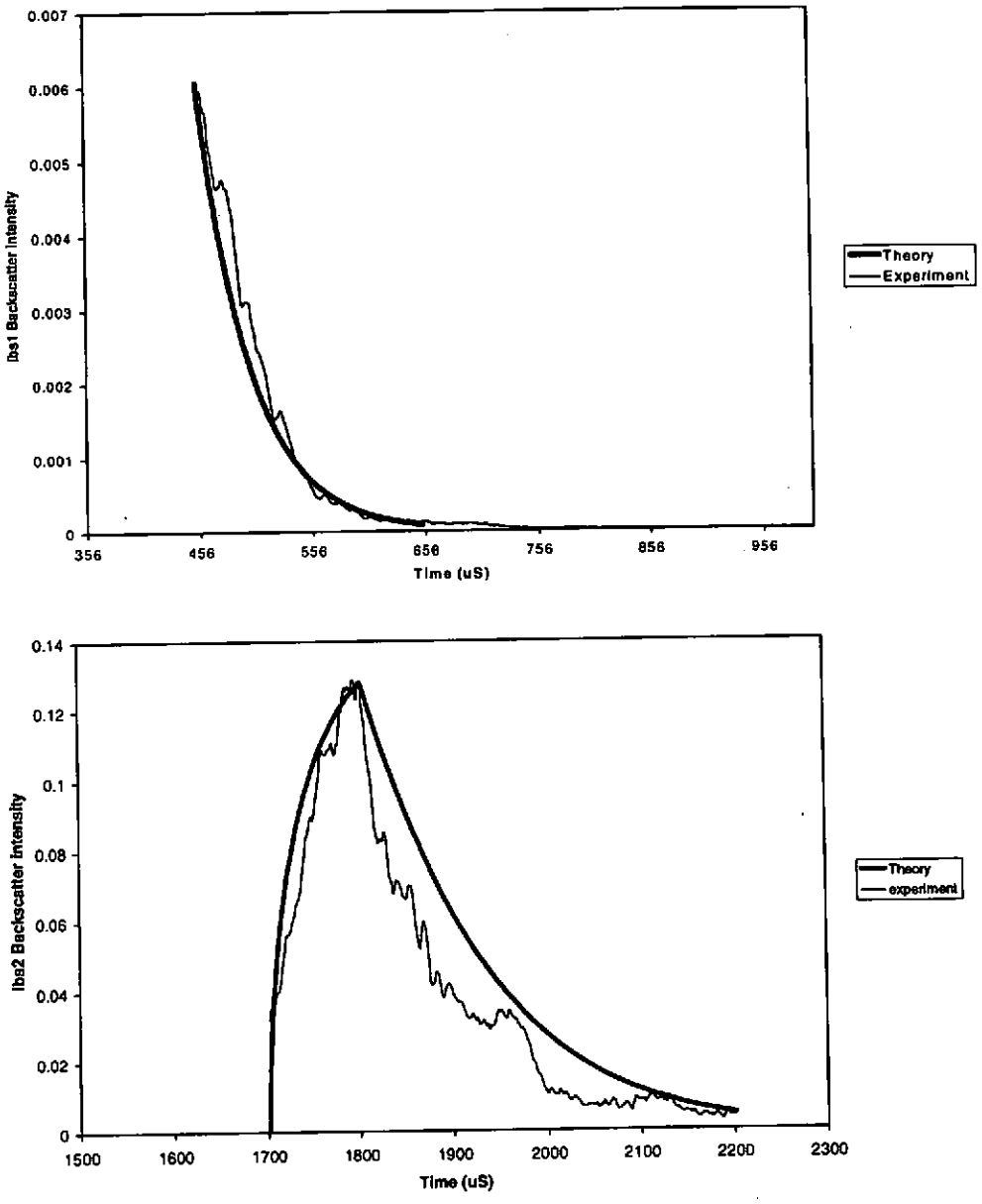

Figure 5. Graph showing the tail of the first backscatter (top) and the whole of the second backscatter envelope (bottom) from the gravel with small waves and the theoretical prediction overlaid.

4. Results

The results shown in Figure 6 to 8 show the E_2 against E_1 for the three different wave conditions. Each graph includes the E_1 and E_2 values obtained from the three sediments. It is interesting to note that the discrimination for the flat water case is very poor (Figure 6) and that the discrimination increases as the water surface roughness increases. Chivers has commented that the RoxAnn system seems to perform better in higher sea-states and this is also suggested by the theory presented in Section 2. It is quite probable that the system has not been used in

perfectly flat conditions as the sea surface is very seldom totally calm and even the motion of the host vessel would produce waves in the area of interest.

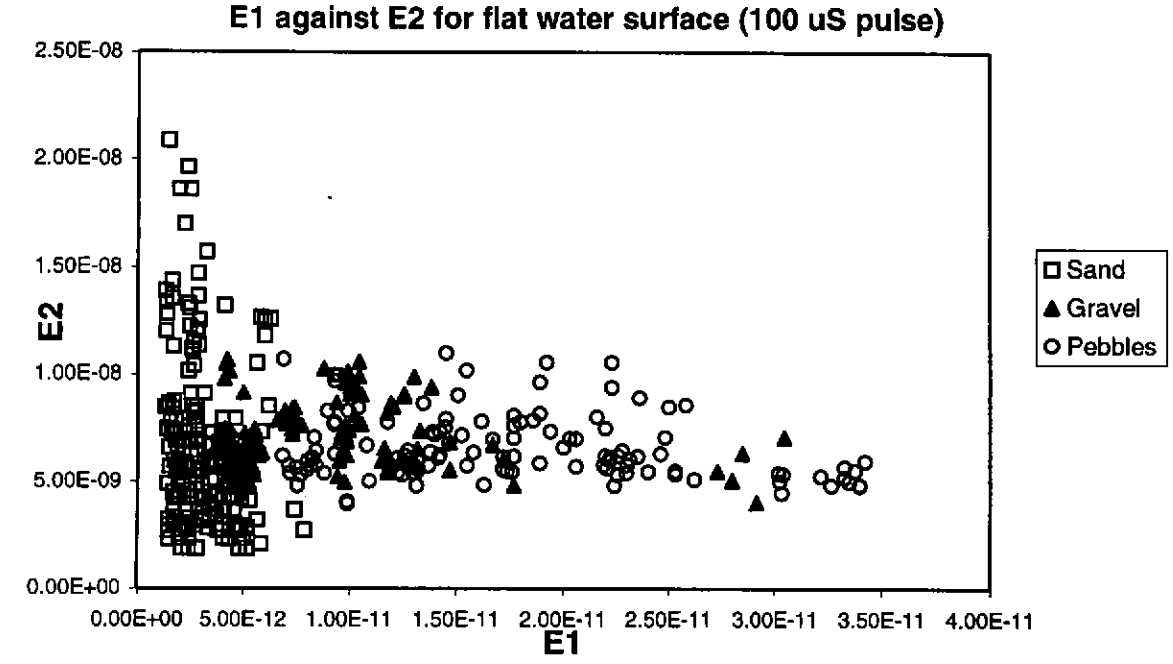

Figure 6. Graph of E_2 against E_1 with a flat water surface showing the values from the three sediments

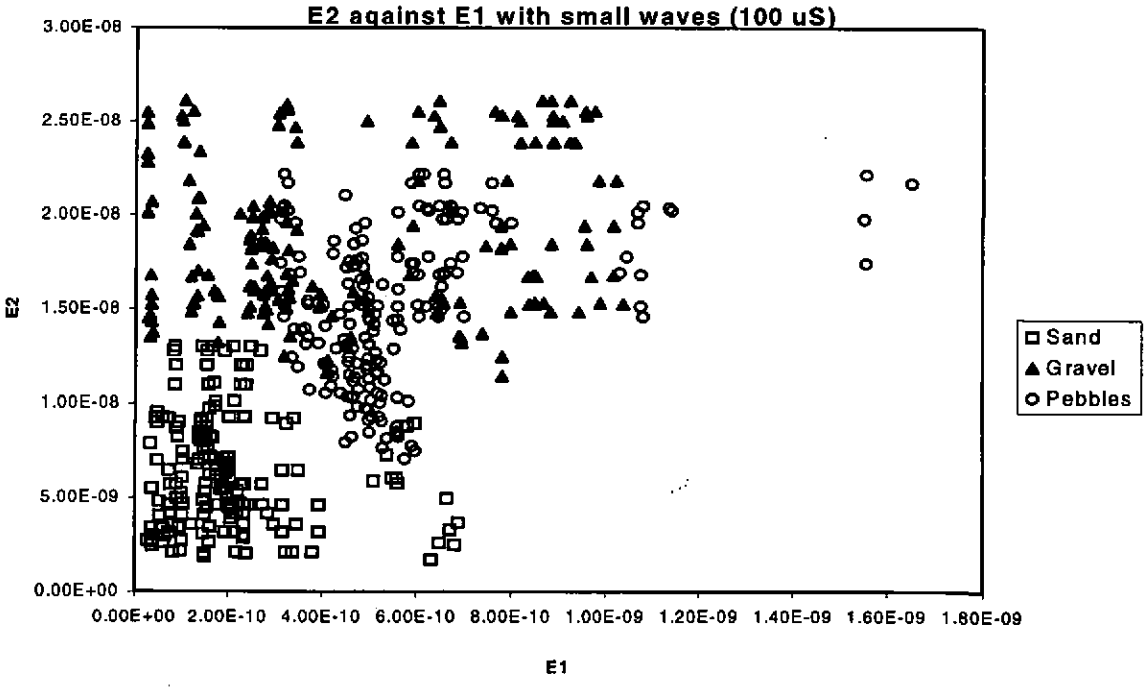

Figure 7. Graph of E_2 against E_1 with a small surface waves showing the values from the three sediments

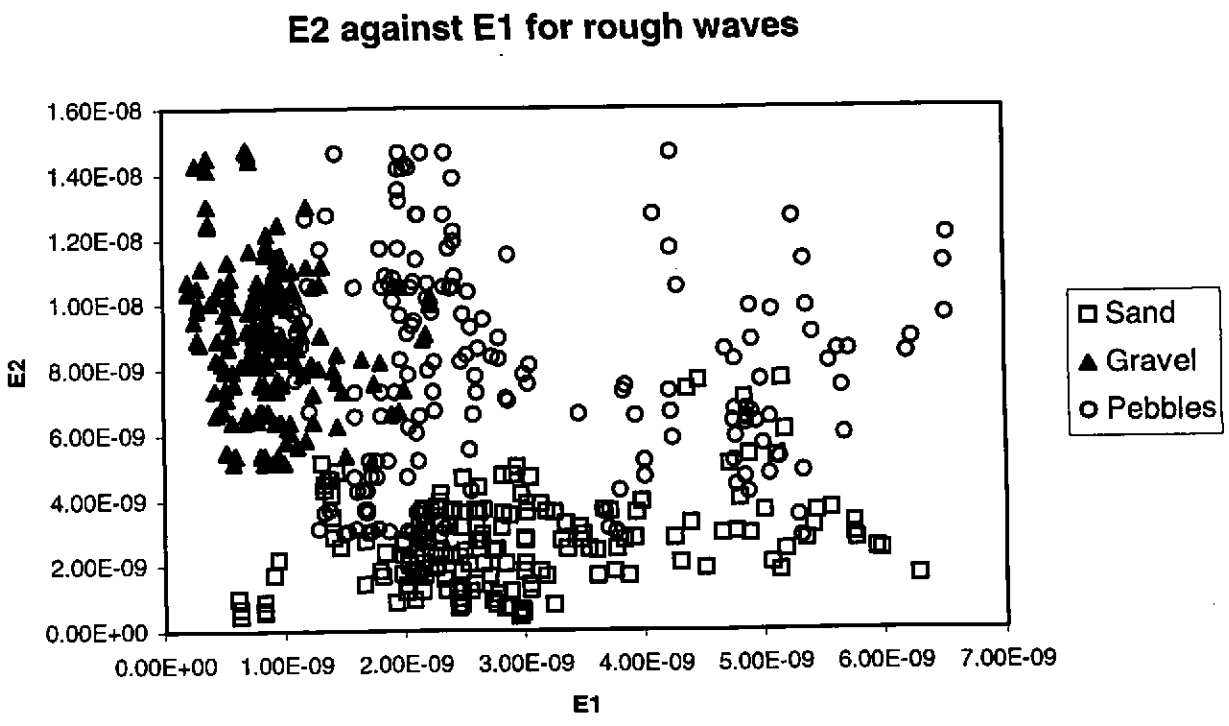

Figure 8. Graph of E_2 against E_1 with large surface waves showing the values from the three sediments

5. Conclusions

The theory presented in Section 2 shows that the second backscatter must be treated in terms of an on-axis bistatic geometry and it is shown that this is also the reason why the second echo contains additional information. It is also shown that the spreading due to the water surface is an important part of the mechanism and the increased insonified area enhances the effect. The time series results from the tank experiment show good agreement with the theoretical prediction for both the first and second backscatter. This also gives confidence that the theoretical values of E_1 and E_2 would be representative.

The graphs of E_2 against E_1 show that the discrimination, when the water surface is flat, is very poor but improves when waves are added to the water surface. It is worth noting that in the range-dependence research by Pace *et al.* [5] a R1/R2 ratio of only three would mean that the receiver is starting to move away from the far-field region but it would not be sufficient to place it in the near field of the scatter. The enhancement due to the water surface roughness is demonstrated in both the theory and the experimental results.

6. Acknowledgements

The author would like to thanks Dr N.G.Pace, Dr P.C.Hines, Dr V.F.Humphrey and Ms C.M.Dyer for their input and scientific discussion during this research.

References

[1] Chivers RC, Burns DR and Emerson N. New acoustic processing for underway surveying, *The Hydrographic Journal*, 1990; No. **56**.

[2] Emerson N, Chivers RC and Burns DR. D.I.Y ground discrimination and much much more! *Proc. Advances in Underwater Technology, Ocean Science and Offshore Engineering*, 17 Oceanology International 90, Publ Graham and Trotman, London, 1990.

[3] Burns DR, Queens CB and Chivers RC. Ground and fish discrimination in underwater acoustics, *Proc. Ultrasonics International 85* pp 49-52 IPC Press Guildford, 1985.

[4] Orlowski A. Application of multiple echoes energy measurement for evaluation of sea bottom type, *Oceanologica* , 1984; 19.

[5] Pace NG, Al-Hamdani ZKS and Thorne PD. The range dependence of normal incidence acoustic backscattering from a rough surface, *Journal of the Acoustical Society of America*, 1985; 77: 101–112.

[6] Hines P.C. and Heald G.J. (2001), Seabed classification using normal incidence backscatter measurements in the 1-10 kHz frequency band, in *'Acoustical Oceanography', Proceedings of the Institute of Acoustics Vol. 23 Part 2, 2001,* T G Leighton, G J Heald , H Griffiths and G Griffiths, (eds.), Institute of Acoustics, (this volume), pp. 42-50.

[7] Brekovskikh LM and Lysanov YuP. *Fundamentals of Ocean Acoustics*, Springer-Verlag. 1988.

[8] Pace NG. Acoustic backscatter and seabed characteristics, *Proceedings of the Institute of Acoustics, Vol 12 Part 1*, 1990, pp 21 – 31.

[9] Heald G.J. (2000), An analysis of normal incidence acoustic backscatter for seabed discrimination, *PhD Thesis – University of Bath*